Minimization of machine and inverter losses in hybrid excited machines for electric vehicles

M. Bonislawski, M. Holub and R. Palka

Department of Electrical Engineering
West Pomeranian University of Technology
Sikorskiego 37, 70-313 Szczecin, Poland
phone: +48 91 449 48 73, fax: +48 91 449 43 17
e-mail: Michal.Bonislawski@zut.edu.pl, Marcin.Holub@zut.edu.pl, Ryszard.Palka@zut.edu.pl

Abstract

This paper discusses a control system for a hybrid excited permanent magnets synchronous machine (HPMSM) with a stator based field coil, meant to achieve the maximum efficiency of the inverter-machine system. Losses in the HPMSM have been divided into some separate categories: copper losses (in the windings), core losses (in the magnetic circuit), mechanical losses, losses in structural elements and different power inverter losses (conduction and switching). Several different loss calculation algorithms have been analysed and taken into account. The torque equation of a hybrid excited PMS-machine has been modified in order to evaluate the efficiency optimal control method. The experiment results clearly exhibit the benefits of the proposed approach.

Key words

Electrical vehicles, hybrid machines, field weakening, control of machines, power losses

1. Introduction

Internal combustion engines are the predominant propulsion and power sources in passenger vehicles, utility vehicles and ships. Key air pollutants emitted from combustion engines in all modes of transport include nitrogen oxides, sulphur oxides, particulate matter, carbon monoxide and volatile organic compounds. Overall, the emission trends in Europe are positive, with a stable greenhouse gas emission reduction, but according to legislation, transport emissions will need to be reduced by 68% by 2050 in order to meet the key target set out by the European Union.

Due to these facts, an increasing number of research and technological efforts is directed to purely electric vehicles. Permanent magnet synchronous machines (PMSM) are often used in their drivetrains, but they are usually limited in terms of their flux weakening range and low-speed torque values. Therefore, hybrid excited PMSM machines are becoming an attractive alternative, especially due to the lack of limitations in excitation field control.

2. Hybrid excited PMS-machine

In order to increase the flexibility of the excitation field control (field weakening), a hybrid machine construction was proposed ([9], [10]). An overview of the proposed solution is presented in Fig. 1. A stator is constructed out of two identical cores separated by an additional excitation coil caring i_{exc} current. The rotor poles are magnetized by groups of four rare-earth magnets.

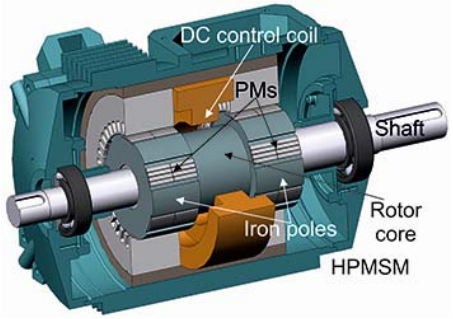

Fig. 1. Construction overview of the HPMSM

The basic parameters of the constructed hybrid machine prototype are summarized in Table 1.

TABLE I. - Main parameters of the HPMSM prototype

Symbol	Parameter	Value
p	Pole pairs	6
L_d	d-axis inductance	5.5 mH
L_q	q-axis inductance	6 mH
R_s	stator resistance	0.3 Ω
L_{exc}	Additional excitation coil inductance	1 H
R_{exc}	Additional excitation coil resistance	8 Ω

Based on the known parameters and voltage-flux equations of a typical PMS-machine, a HPMS-machine model was developed (d-q axis flux equations and the torque equation) [10]:

$$u_d = R_s i_d + L_d \frac{di_d}{dt} + M_{exc} \frac{di_{exc}}{dt} \overbrace{-\omega_e L_q i_q}^{e_d} \qquad (1)$$

$$u_q = R_s i_q + L_q \frac{di_q}{dt} + \overbrace{\omega_e \left(L_d i_d + \psi_{PM} + M_{exc} i_{exc} \right)}^{e_q} \quad (2)$$

where: u_d, u_q – d- and q-axis voltages, i_d, i_q – d- and q-axis currents, R_s – stator phase winding resistance, Ψ_{PM} – magnetic flux of permanent magnets, p – number of pole pairs, T_e – electromagnetic torque, M_{exc} – inductance of the additional excitation coil coupled with the d-axis. Values e_d and e_q are induced voltages in d and q axes, respectively.

It is worth noting that in most models proposed in literature ([12], [13]) the excitation flux exhibits a non-linear dependency on i_{exc}. This also occurs in the case of the investigated prototype, as seen in Fig. 2. Overlooking this fact might lead to improper i_{exc} current distribution and false excitation values.

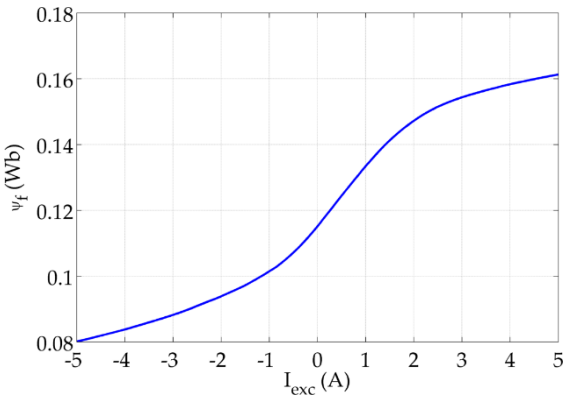

Fig. 2. Excitation coil current iexc – excitation flux ψ_f characteristics of investigated prototype

The torque equation of a hybrid excited PMS-machine can be written as:

$$T_e = \frac{3}{2} p \left(i_q \psi_d - i_d \psi_q \right) = \\ = \frac{3}{2} p \left[\overbrace{\psi_{PM} i_q}^{T_{sync}} + \overbrace{M_{exc} i_{exc} i_q}^{T_{exc}} + \overbrace{\left(L_d - L_q \right) i_d i_q}^{T_{rel}} \right], \quad (3)$$

where: Ψ_d, Ψ_q – d- and q-axis magnetic fluxes.

Three components constituting torque production can be noticed: the synchronous torque T_{sync} proportional to the q axis current and the (constant) excitation flux of permanent magnets, T_{exc} – a characteristic component of hybrid excitation machines, proportional to the excitation current i_{exc}, T_{rel} – reluctance torque resulting from the magnetic asymmetry of HPMS-machine construction.

3. Machine losses

Losses in the HPMSM can be divided into some separate categories: copper losses (in the windings), core losses (in the magnetic circuit), mechanical losses and losses in all other structural elements. Based on the equation presented above, it can be concluded that a certain torque value can be obtained using different (i_d, i_q) current combinations with different values of the excitation coil current i_{exc}. This raises questions in regards to the optimal current component distributions for different optimization goals. A natural and common optimization goal is the overall system efficiency improvement. In order to achieve these target loss mechanisms, on needs to perform an analysis and present a mathematical description of loss.

Copper losses can be described as summarized losses of stator windings and losses stemming from the additional inductance L_{exc} excitation. Therefore, the following formula can be proposed:

$$P_{cu} = \frac{3}{2} R_s \left(i_d^2 + i_q^2 \right) + R_{exc} i_{exc}^2 \quad (4)$$

where R_{exc} is the resistance of the additional excitation coil.

In addition, magnetization losses are connected to the cyclic iron lamination field change and can be traced back to two important contributors: the hysteresis losses of the material and the eddy current losses on lamination edges. For sinusoidal magnetic flux density B, both can be described using an empirical equation [14]:

$$P_c = k_h \omega_e B_{pk}^{\beta} + k_{ed} \omega_e^2 B_{pk}^2 \quad (5)$$

where k_h is the hysteresis loss coefficient, β is the Steinmetz coefficient and k_{ed} is the eddy current constant. Summarized magnetic core material losses were included in the model using an equivalent (for a given operating point) resistor R_c. Due to the problematic procedures of material constants, an experimental approach is often used [15]. R_c is calculated using the formula for summarized core losses P_c:

$$R_c = \frac{3}{2} \frac{\left(\omega_e \psi_s \right)^2}{P_c} \quad (6)$$

The overall HPMSM model, with core loss dependent resistance R_c is depicted in Fig. 3.

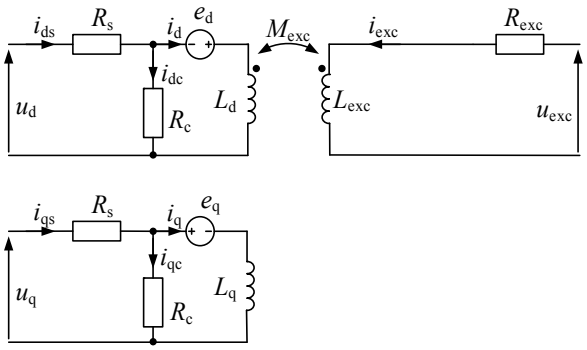

Fig. 3. HPMS-machine model with core loss dependent resistance R_c

Simplified methods for determining the value of R_c are based on the experiment where the shaft of the tested HPMSM is driven (by auxiliary motor) and the

mechanical power provided for different speeds is measured. Measured mechanical losses allow the separation of their individual components (at the constant speed the change of flux linkage affects the level of core losses only).

4. Power inverter losses

Regarding the power electronic system schema a 6 IGBT transistor full bridge inverter was used with a 4 transistor, full bridge excitation coil control, as in Fig. 4.

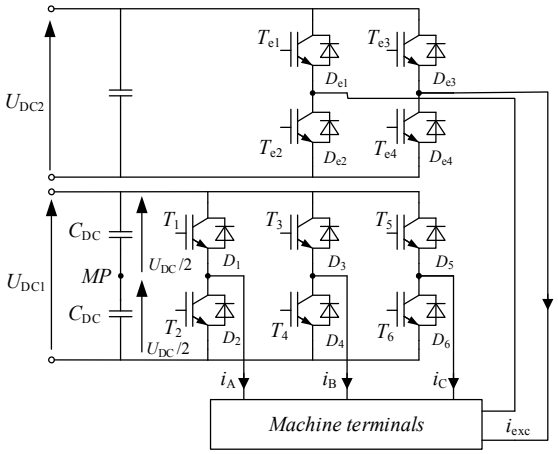

Fig. 4. HPMSM power electronic system

As can be noticed 10 IGBT transistors and 10 power diodes contribute to losses, two independent DC links exist. Because the excitation coil is driven by low-voltage transistors with very high efficiency this part of losses was neglected resulting in loss estimation necessity for 6 power transistors and 6 power diodes. The time-domain calculation of losses for all possible points of load would be very time-consuming, therefore an alternative approach was taken. Based on the transistor and diode documentation (SK60GB123 documentation was used), a Piecewise Cubic Hermite Interpolating Polynomial interpolation was used for transistor and diode voltage drop and switching energies for junction temperature of 125°C. Examples of the results are presented in Fig. 5 and Fig. 6.

Based on interpolated characteristics of conduction and switching (only turn-off losses of diodes were incorporated), individual losses were calculated according to the following formulas, respectively:

$$P_{\mathrm{Tcond}} = \frac{1}{T_{\mathrm{ref}}} \int_0^{T_{\mathrm{ref}}} i_{\mathrm{c}}(t) u_{\mathrm{ce}}(t) \mathrm{d}t \tag{7}$$

$$P_{\mathrm{Dcond}} = \frac{1}{T_{\mathrm{ref}}} \int_0^{T_{\mathrm{ref}}} i_{\mathrm{D}}(t) u_{\mathrm{Df}}(t) \mathrm{d}t \tag{8}$$

$$P_{\mathrm{Tswon}} = \frac{1}{n} \sum_{j=1}^{n} E_{\mathrm{Ton}}(j) \tag{9}$$

$$P_{\mathrm{Tswoff}} = \frac{1}{n} \sum_{j=1}^{n} E_{\mathrm{Toff}}(j) \tag{10}$$

$$P_{\mathrm{Dswoff}} = \frac{1}{n} \sum_{j=1}^{n} E_{\mathrm{Doff}}(j) \tag{11}$$

Examples of calculation results of transistor and diode losses for a single operating point are presented in Fig. 7 (f_{cr} – carrier waveform frequency, f_{ref} – reference voltage frequency, m – amplitude of the reference voltage). It should be noted that often used semiconductor loss calculation methods assume simplified conduction voltage drop and switching energy characteristics, which might lead to erroneous power loss estimation.

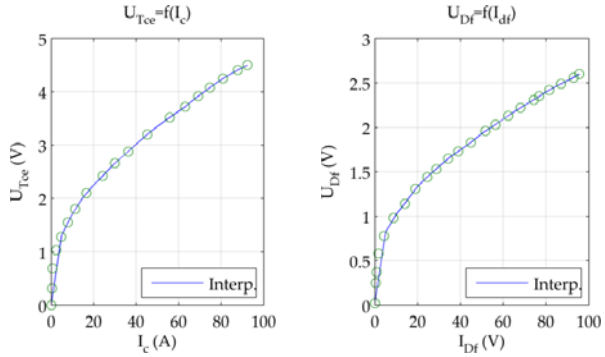

Fig. 5. IGBT transistor (left) and diode (right) conduction characteristics

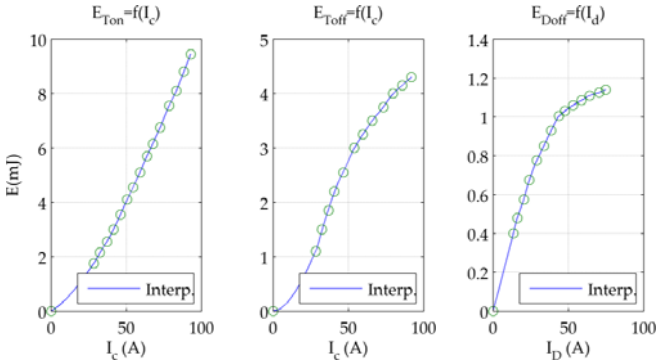

Fig. 6. Switching energy of IGBT transistors (E_{Ton}, E_{Toff}) and power diodes (E_{Doff})

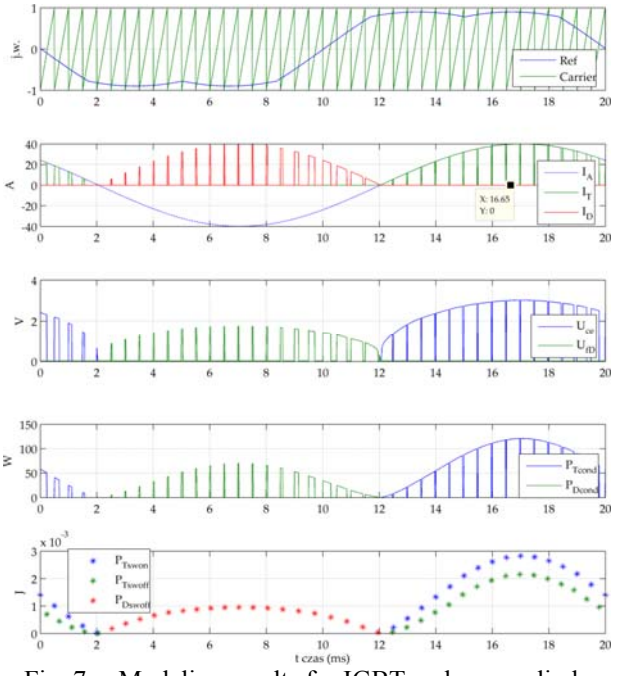

Fig. 7. Modeling results for IGBT and power diode losses according to formulas (7-11) for modulation frequencies $f_{\mathrm{ref}} = 50\mathrm{Hz}$; $f_{\mathrm{cr}} = 2\mathrm{kHz}$; $I_{\mathrm{A(max)}} = 40\mathrm{A}$; $\cos\varphi = 0.7$; $m = 0.9$

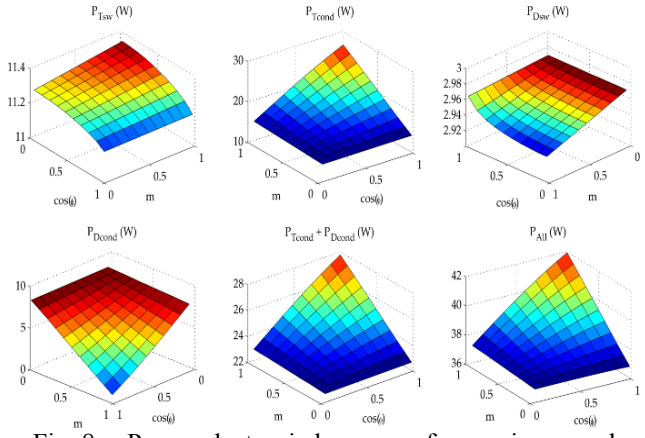

Fig. 8. Power electronic loss maps for varying m and cosφ, stator current of 35 A

Based on the approach proposed above and overall losses for all combinations of machine current amplitudes, modulation depth indexes m and machine cosφ were calculated. Examples of loss maps for the switching frequency of 10 kHz and the stator current of 35 A are depicted in Fig. 8. The proposed loss calculation method was compared to time-domain simulations proving an error of max. 10 %.

5. Loss minimization algorithms

Although broadly used in PMSM, control loss minimization algorithms are not as widely used in HPMSM. One of the first approaches to optimize an HPMSM machine was introduced in [16]. A fuzzy logic based approach was used to calculate optimal stator and excitation coil currents. An improved efficiency of the motor was reported with the maximum efficiency of 92%. Inverter and motor loss analysis was not performed. Copper and combined copper-iron losses were analytically minimized in [17]. An extended Lagrange multiplier optimization method was used (with Kuhn-Tucker conditions) to elaborate optimal stator and excitation coil currents in different regions of operation. A simulation-based validation is described with copper losses minimization, no power electronics losses are considered. A self-searching approach was proposed in [18], however only the additional excitation coil current is varied experimentally, with no a priori knowledge of the results and no perturbation of stator currents. The combined inverter machine losses are minimized. Another approach is to use iterative particle swarm optimization and fuzzy control [19]. Iron losses and power electronic unit losses were neglected in the proposed study; in regards to the copper loss, simulations reported an advantage of 22%. Yet another possibility is to utilize an algorithm with pre-calculated look-up table stored currents, depending on the speed and torque command, as was often done for PMSM machines [20].

6. Control system of the HPMSM

The starting point of the proposed approach is the evaluation of efficiency maps for the power electronic converter and the machine, including mechanical, iron and copper losses.

After calculating the power electronic losses, machine efficiency maps for all possible torque-angular speed points were calculated for iteratively varied I_{exc}, I_d and I_q. It must be emphasized that both the mechanical friction based torque and the mechanical power loss were also taken into account. The R_c value was interpolated from experimental data (as a function of rotor speed and excitation flux). Operation point stator, coil currents and voltages were calculated using formulas (1) and (2) in order to calculate all losses. Following this operation and based on the resulting operation point maps, elements exceeding maximum allowable voltage and/or current values are eliminated. These operations were performed for all I_{exc}, I_d and I_q combinations. An additional analysis is carried out in connection with the power electronics loss mapping. Overall, the (conduction and switching) losses are calculated for all necessary inverter operating points. Finally, having all the efficiency maps of the machine and the power converter, an overall efficiency marker is calculated for every current combination.
An additional analysis is carried out in connection with the power electronics loss mapping. Overall losses are calculated for all necessary inverter operating points, as functions of U_{AB}, $I_{s(RMS)}$, cos(φ). Finally, having all the efficiency maps of the machine and the power converter, the overall efficiency maps are established for all current combinations leading to maximized system efficiency.

7. Experimental results

In order to examine the practical properties of the proposed approach an experimental test-stand was constructed. The HPMSM machine prototype was constructed having the parameters listed in Table 1. A servo IM drive from ABB was used as a dynamic load. Power electronics, controller board and power equipment are presented in Fig. 9.

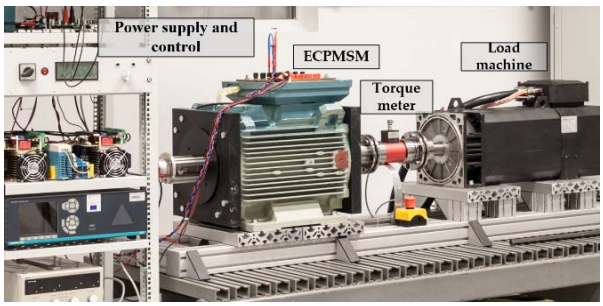

Fig. 9. Power supply and monitoring unit with DSP-based controller

A broad experimental program was carried out in order to verify the benefits of the overall proposed optimization procedure. Optimization results and different optimization loss components were also examined using standardized drive cycle NEDC modeling.

8. Conclusion

A power inverter-HPMSM loss minimization iterative procedure was described leading to “a-priori” look-up-table based, optimal controller. Proposed approach includes a non-linear character of excitation flux as a

function of additional coil current, experimental description of material properties for core loss calculation and an adequate model of power transistor and power diodes energy loss characteristics with linear interpolation. Off-line, iterative algorithm limits necessary calculation time and necessary processor power, allows for flexible analysis of sensitivity and distribution of results as a function of various parameter variations.

Experimental results clearly exhibit the benefits of proposed approach. Optimization results were implemented, as look-up-tables in the memory of the control unit. A decrease of up to 6% of overall system losses was measured, mostly in the high speed range of the machine.

Acknowledgement

This work has been supported with the grant of the National Science Centre, Poland 2015/17/B/ST8/03251.

References

[1] European Environment Agency, "A closer look at urban transport", EEA Report No. 11/2013, ISSN 1725-9177.

[2] European Environment Agency, "The contribution of transport to air quality", EEA Report No. 10/2012, ISSN 1725-9177.

[3] P. Paplicki, M. Wardach, M. Bonislawski, R. Palka, "Simulation and experimental results of hybrid electric machine with a novel flux control strategy", Archives of Electrical Engineering, Vol. 64(1), 2015, pp. 37-51.

[4] M. Bonislawski, R. Palka, P. Paplicki, M. Wardach, "Unconventional control system of hybrid excited synchronous machine", Proceedings of the 20th Int. Conference on Methods and Models in Automation and Robotics: MMAR 2015, pp. 649-654.

[5] M. Bonislawski, R. Palka, "Efficiency Optimal Control System of Hybrid Excited Machines", Proceedings of the 21st Int. Conference on Methods and Models in Automation and Robotics: MMAR 2016, in press.

[6] P. Putek, P. Paplicki, R. Palka, "Low cogging torque design of Permanent-Magnet machine using modified multi-level set method with total variation regularization", IEEE Trans. Magn. Vol. 50, No. 2, 2014.

[7] P. Putek, P. Paplicki, R. Palka, "Topology optimization of rotor poles in a permanent-magnet machine using level set method and continuum design sensitivity analysis", Compel, The International Journal for Computation and Mathematics in Electrical and Electronic Engineering, Vol. 33, No. 3, 2014, pp. 711-728.

[8] P. Putek, M. Slodička, P. Paplicki and R. Palka, "Minimization of cogging torque in permanent magnet machines using the topological gradient and adjoint sensitivity in multi-objective design", International Journal of Applied Electromagnetics and Mechanics, Vol. 39 No. 1-4, 2012, pp. 933-940.

[9] P. Di Barba, M.E. Mognaschi, R. Palka, P. Paplicki, S. Szkolny, "Design optimization of a permanent-magnet excited synchronous machine for electrical automobiles", International Journal of Applied Electromagnetics and Mechanics, Vol. 39, No. 1-4/2012, pp. 889-895.

[10] P. Di Barba, M. Bonislawski, R. Palka, P. Paplicki, M. Wardach, "Design of Hybrid Excited Synchronous Machine for Electrical Vehicles", IEEE Transactions on Magnetics, Vol. 51, No. 8, August 2015.

[11] G. Slemon and R. Bonert, "Modeling of iron losses of permanent-magnet synchronous motors", IEEE Transactions on Industry Applications, vol. 39, no. 3, pp. 734–742, May 2003.

[12] J.A. Tapia, F. Leonardi, and T.A. Lipo, "Consequent -pole permanent-magnet machine with extended field-weakening capability", IEEE Transactions on Industry Applications, vol. 39, no. 6, pp. 1704–1709, 2003.

[13] Z. Zhang, Y. Yan, S. Yang, and Z. Bo, "Principle of Operation and Feature Investigation of a New Topology of Hybrid Excitation Synchronous Machine", IEEE Transactions on Magnetics, vol. 44, no. 9, pp. 2174–2180, 2008.

[14] G. Slemon and R. Bonert, "Modeling of iron losses of permanent-magnet synchronous motors", IEEE Transactions on Industry Applications, vol. 39, no. 3, pp. 734–742, May 2003.

[15] N. Urasaki, T. Senjyu, and K. Uezato, "A novel calculation method for iron loss resistance suitable in modeling permanent-magnet synchronous motors", IEEE Transactions on Energy Conversion, vol. 18, no. 1, pp. 41–47, Mar. 2003.

[16] C. Chan, R. Zhang, K. T. Chau, and J. Z. Jiang, "Optimal efficiency control of PM hybrid motor drives for electrical vehicles", Power Electronics Specialists Conference, 1997. PESC '97 Record., 28th Annual IEEE, 1997, vol. 1, pp. 363–368.

[17] R. Mbayed, G. Salloum, L. Vido, E. Monmasson, and M. Gabsi, "Hybrid excitation synchronous motor control in electric vehicle with copper and iron losses minimization", IECON 2012 - 38th Annual Conference on IEEE Industrial Electronics Society, 2012, pp. 4886–4891.

[18] K.T. Chau, "Efficiency Optimization of a Permanent-Magnet Hybrid Brushless Machine Using DC Field Current Control", IEEE Transactions on Magnetics, vol. 45, no. 10, pp. 4652–4655, Oct. 2009.

[19] M. Huang, H. Lin, H. Yunkai, P. Jin, and Y. Guo, "Fuzzy Control for Flux Weakening of Hybrid Exciting Synchronous Motor Based on Particle Swarm Optimization Algorithm", IEEE Transactions on Magnetics, vol. 48, no. 11, pp. 2989–2992, Nov. 2012.

[20] J. Lee; K. Nam; S. Choi; S. Kwon, "Loss-Minimizing Control of PMSM With the Use of Polynomial Approximations", IEEE Transactions on Power Electronics, vol. 24, no. 4, pp. 1071,1082, April 2009.